Research Article

Xiangsheng Gao*, Kuan Zhang, Min Wang, Tao Zan, Peng Gao, and Chaozong Liu

Optimization of nano coating to reduce the thermal deformation of ball screws

https://doi.org/10.1515/ntrev-2022-0029
received November 1, 2021; accepted December 27, 2022

Abstract: To reduce the thermal deformation of ball screws, the process of nano coating preparation for coating on ball screws to reduce temperature rise and thereby thermal deformation was discussed in this article. Simultaneously, the cooling mechanism was presented. The thermal channels and the relatively even distribution of graphene in the nano coating were observed in scanning electron microscopic images. In terms of the preparation of nano coating, optimization design was carried out to obtain the optimized material ratio and nozzle flow through orthogonal experiment. The influence of design parameters of nano coating on reducing thermal deformation was also discussed. The experimental results show that the maximum temperature rise, thermal deformation, and time to reach thermal balance decreased by 12.5, 69.1, and 46.3%, respectively. The effectiveness of nano coating in reducing thermal deformation was validated experimentally.

Keywords: ball screw, nano coating, thermal deformation, graphene

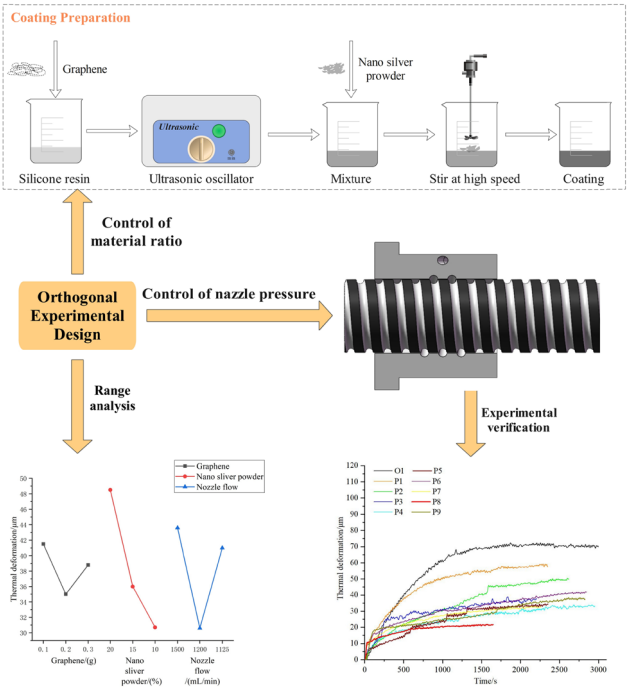

Graphical abstract

1 Introduction

Ball screws play an important role in accuracy stability of machine tools based on their high efficiency and good stiffness. However, their accuracy is affected by temperature rise caused by the heat sources of machine tools. Previous studies show that errors caused by thermal factors of machine tools account for 40–70% of the total errors [1]. Thus, the thermal error of machine tools can be reduced by presenting a ball screw with improved thermal performance. And studying on thermal performance of ball screws has attached much attention to improve the positioning accuracy of machine tools.

Thermal error compensation is an effective measure to deal with the decrease in ball screw positioning accuracy. Thermal error modeling is the key factor in the thermal error compensation. In terms of thermal error modeling, there are usually two methods, finite element method (FEM) and data-driven method. Liu *et al.* [2] investigated the dynamic behavior of adjustable preload double-nut ball screw using finite element simulation and experiments. Li *et al.* [3] used FEM to simulate temperature fields of ball screw feed drive system. FEM is

* **Corresponding author: Xiangsheng Gao,** Beijing Key Laboratory of Advanced Manufacturing Technology, Faculty of Material and Manufacturing, Beijing University of Technology, Beijing 100124, China, e-mail: gaoxsh@bjut.edu.cn, tel: +86-10-6739-2137
Kuan Zhang, Min Wang, Tao Zan, Peng Gao: Beijing Key Laboratory of Advanced Manufacturing Technology, Faculty of Material and Manufacturing, Beijing University of Technology, Beijing 100124, China
Chaozong Liu: Division of Surgery and Interventional Science, University College London, Royal National Orthopaedic Hospital, London HA74LP, United Kingdom

widely used for simulation and analysis. Xie *et al.* [4] studied the mechanical properties of the composite sandwich matting through finite element analysis and experiments. FEM is an effective method in thermal error modeling, but it is difficult to be implemented in online thermal error compensation due to the low modeling efficiency. Li *et al.* [5] established a real-time prediction model of axial thermal error. Li *et al.* [6] presented a real-time prediction method of thermal errors of screw system based on an adaptive moving thermal network model. Chen *et al.* [7] proposed a thermal error method of the screw-nut feed system considering the heat transfer distance. Gao *et al.* [8] established the prediction model of thermal errors using PSO-LSTM neural network. Yang *et al.* [9] utilized the improved Elman network to carry out the thermal error modeling. Li *et al.* [10] established a finite difference heat transfer model to obtain the temperature field of the screw. Zapłata and Pajor [11] presented a compensation method of thermal errors using partial differential equation model. Li *et al.* [12] established an adaptive online analytical compensation model to compensate the positioning error of ball screw feed drive systems. Liu *et al.* [13] proposed a data-driven thermal error compensation model for high-speed and precision five-axis machine tools. The accurate models have a positive effect on reducing thermal errors.

Thermal error suppression is another measure for improvement of ball screw positioning accuracy. Ju *et al.* [14] proposed a method to suppress the thermal error by using an oil cooling system. Additionally, Shi *et al.* [15] investigated the effect of cooling system parameters and cooling medium flow rate on temperature distribution of screw shaft of feed drive system. Besides, many materials with unique properties were also used in thermal error reduction and accuracy improvement. Voigt *et al.* [16] designed a latent heat storage unit based on phase change materials (PCMs) to reduce temperature fluctuation. In our previous work ref. [17], a novel ball screw based on inner-embedded carbon fiber reinforced plastic (CFRP) was designed to reduce thermal deformation, and the effectiveness was validated under actual working condition [18]. In order to improve the thermal conduction between the screw and CFRP, a thermal conductor was mounted between them [19]. Although our previous method for improving ball screws is effective, the design is difficult to be implemented in engineering practice due to the high cost of high-modules carbon fiber and the difficulties in manufacturing. As for the improved ball screw manufacturing, 3D printing is not suitable for it. On one hand, due to the residual stress caused by 3D printing, the size will not be stable leading to inaccurate positioning. On the other hand, the raceway of ball screws by 3D printing cannot be guaranteed to be smooth to ensure the perfect ball-raceway contact. And the thermal management of coating is an effective way to reduce temperature, which has a potential application on ball screws due to the low cost and easy manufacturing. Japar *et al.* [20] reviewed the designs of microchannel heat sink with channel designs that could result in a high heat transfer rate. Bhat *et al.* [21] reported that the thermal diffusivity of coating was improved by using the carbon nanotubes. Zheng *et al.* [22] introduced the development of transparent nanomaterial-based solar cool coatings to reduce solar heat gain into the buildings. Chen *et al.* [23] exploited an efficient passive cooling coating with good cooling effect. Cheng *et al.* [24] proposed a single-layer radiative cooling coating, and the best cooling performance was obtained. Niazi *et al.* [25] developed a technique of microbial bio-coating surface modification for thermal-fluid applications. Sivanathan *et al.* [26] summarized that the heat transport rate can be improved by PCMs encapsulation. Zhang *et al.* [27] concluded that the thermochromic coatings can reduce the annual energy consumption. Yi *et al.* [28] designed the heat-reflective coatings to reduce the asphalt pavement temperature, and the cooling effect was tested. Wang *et al.* [29] investigated the effect of five types of coatings using a new data optimization method. Chen *et al.* [30] proposed a three-layer cool coating for asphalt pavements. Tarawneh *et al.* [31] enhanced the heat conduction of epoxy resin by incorporating the polyaniline and graphene nanoplatelets. Chen *et al.* [32] investigated the enhancement mechanism of graphene oxide doping on the heat transfer characteristics of the composite anti-/deicing components. Chen *et al.* [33] considered the effects of polymer materials, coating thicknesses, and surface microstructures on the cooling performance of coatings. Du *et al.* [34] reviewed that the thermal conductivity of cement can be enhanced by incorporating graphene. Cheng *et al.* [35] studied the influence of factors on spectral radiative characteristics of the radiative-cooling coating, which can greatly affect the cooling effect. Kolas *et al.* [36] carried out the measurement related to cooling function of eight different color coatings prepared, and the temperature reduction to 11.5°C was obtained. Zhang and Fan [37] designed a composite coating used to reduce the temperature at the surface of heat source. Kang *et al.* [38] prepared the coatings with high solar reflectance and strong infrared emittance to realize the daytime radiative cooling. Chen *et al.* [39] reported an all-inorganic phosphoric acid-based geopolymer coating with robust radiative cooling performance. Guo *et al.* [40] designed a ball screw with graphene coating to further reduce temperature rise and

thermal deformation. The effectiveness of the coating was validated, but the experiments were carried out based on the ball screw model rather than the real ball screw. In addition, the parameters optimization of the coating was not considered. Thus, a method to optimize the material ratio and processing of coating is necessary to reduce thermal deformation of ball screws.

In terms of thermal deformation reduction of the ball screw, nano coatings were considered as an effective technical approach. In this study, a parameters optimization method of nano coating was conducted. The effect of material ratio and spraying process on nano coating thermal performance was discussed. Herein orthogonal experiment was carried out on self-design ball screw bench to obtain the coating with optimal material ratio and spraying process, which had better performance in reducing the temperature rise and thermal deformation.

Table 1: Parameters of experimental materials

Materials	Description
Graphene	GDF, 11–15 nm, Jingdun, Shanghai, China
Nano silver powder	300 nm, Yinke, Xingtai, China
Modified acrylic silicone resin	RB-237, Xiyanuo, Wuxi, China

A schematic representation of the study is shown in graphical abstract.

2 Methodology

In this study, a positioning accuracy improvement method was proposed by reducing the temperature rise of ball screws. The nano coating was optimized to enhance the thermal dissipation and applied to reduce the thermal deformation of ball screws.

2.1 Nano coating preparation

The nano coating was developed by modified acrylic silicone resin, graphene, and nano silver powder. The properties of all the materials are shown in Table 1. Considering the excellent thermal conductivity of graphene [41] and the nano silver powder, both of them were selected as the variable to prepare the nano coating. Modified acrylic silicone resin was considered as the matrix. As the active ingredients of nano coating, graphene and nano silver powder were dissolved in the silicone resin. Preparation process is shown in Figure 1. Physical dispersion and chemical modification are the main ways to improve

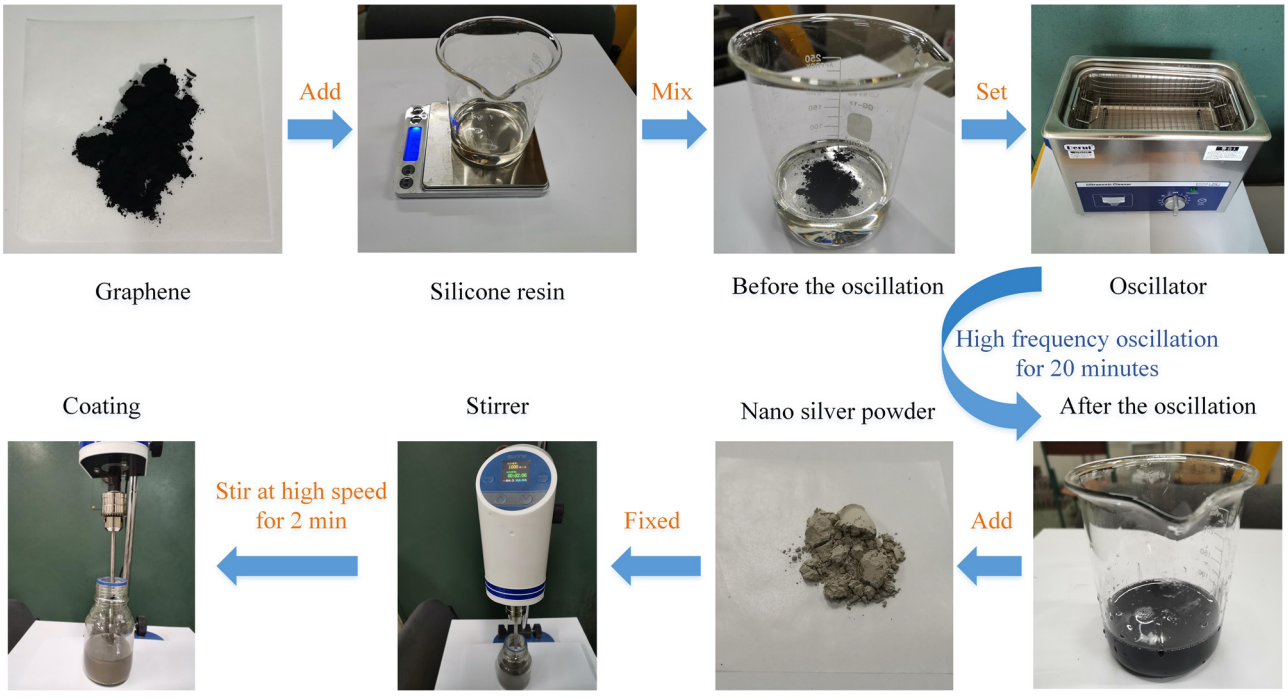

Figure 1: Preparation process of nano coating.

Table 2: Parameters of experimental instruments

Instruments	Product description
High-speed stirrer	SN-OES-60SH, Lichen, Shanghai, China
High-frequency oscillator	DR-MS30, Derui, Shenzhen, China
Electronic scale	CX-12000, Yesheng, Shenzhen, China
Electric spray gun	Pulijie, Hubei, China

Table 3: Parameters of ball screws in test bench

Parameters	Value
Nominal diameter (d_0)	16.8 mm
Lead (l)	10 mm
Material	GCr15

the dispersion of nanomaterials. Ultrasonic dispersion has been regarded as a feasible method to improve the dispersion of graphene oxide [42]. Consequently, ultrasonic dispersion and high-speed stirring were selected to dissolve the graphene and nano silver powder in the silicone resin.

The weighed graphene was added into the beaker after pouring the silicone resin. The mixture was oscillated for 20 min, and the oscillation frequency was set to 40 kHz. After the two were fully mixed uniformly, the nano silver powder was added. The silicone resin, graphene, and nano silver powder were mixed by stirring, and the rotational speed of stirring was maintained at 1,000 rpm for 2 min. An electric spray gun was prepared to spray the graphene nano coating on the surface of the ball screw. During the spraying process, the distance between the nozzle and surface of the ball screw was maintained, and the nozzle pressure was set in advance. After the coating was coated on the whole surface of the ball screw, it was dried for 24 h at ambient temperature. Experiments can be carried out when the coating solidifies and adheres to the surface of the ball screw. During the experiment, the coating on the raceway was destroyed and the rest remained to enhance the heat

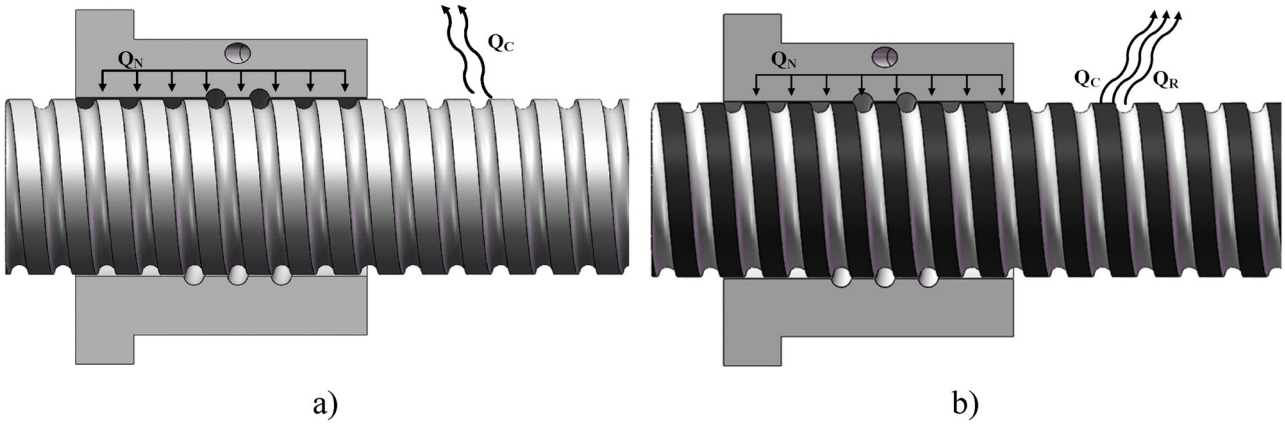

Figure 2: Cooling mechanism. (a) Uncoated ball screw and (b) coated ball screw.

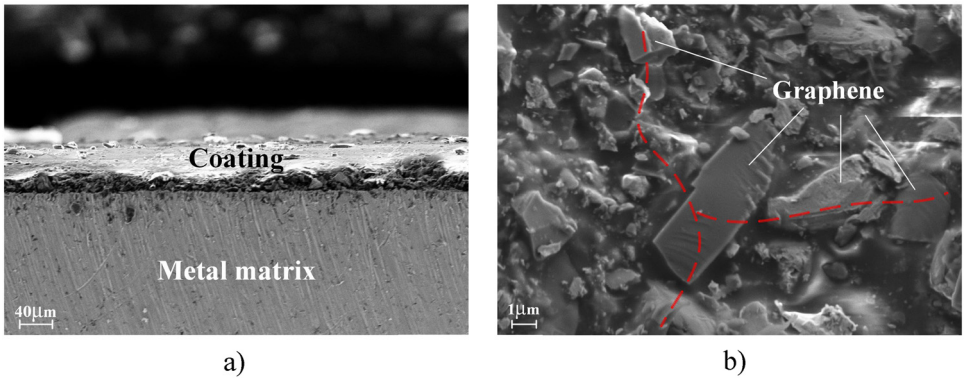

Figure 3: SEM images of the nano coating. (a) State representation and (b) thermal channel formed by grapheme.

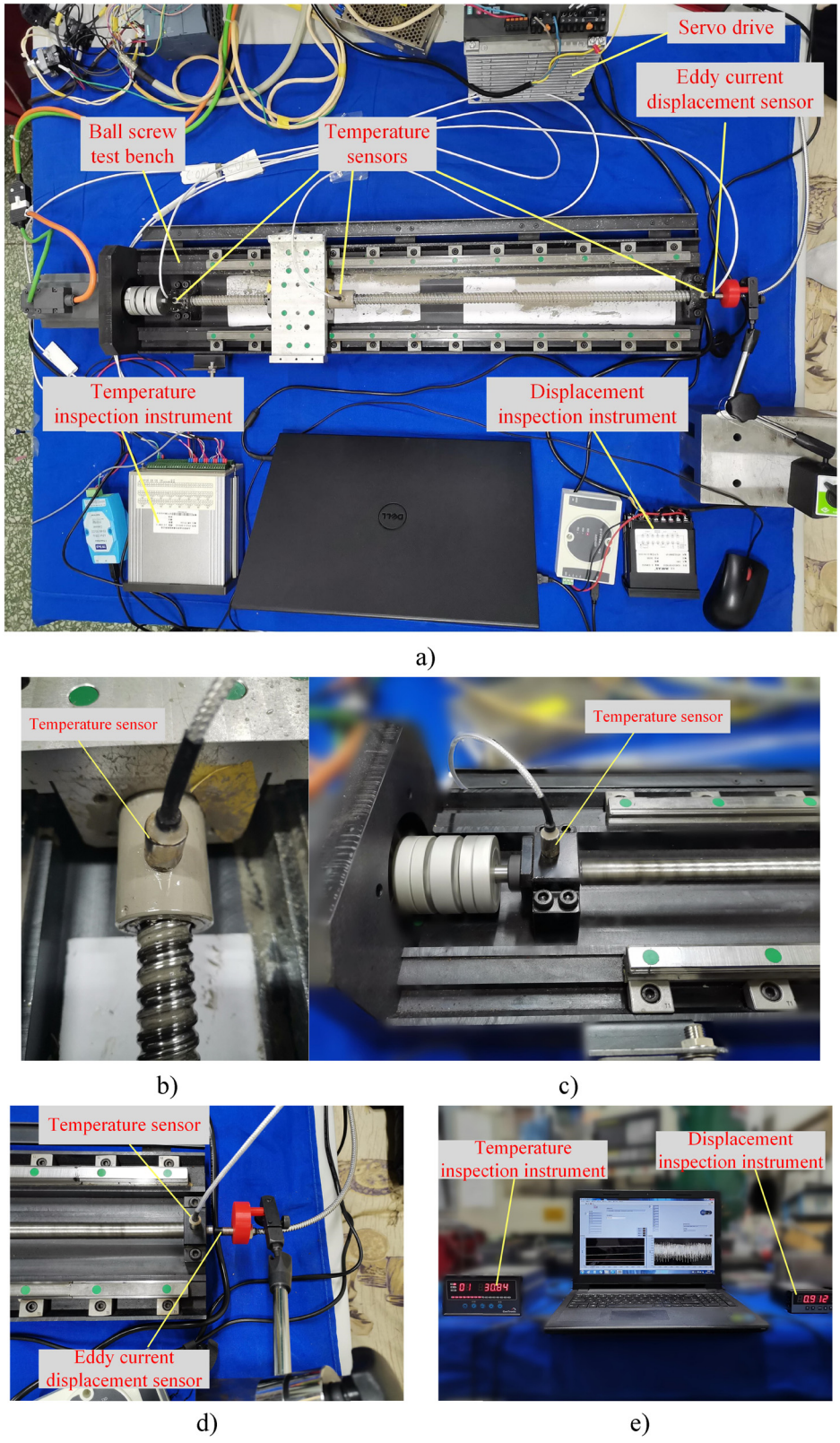

Figure 4: Experimental setup. (a) High speed and precision ball screw test bench, (b) temperature sensor mounted on nut, and (c) temperature sensor mounted on bearing, (d) temperature and thermal deformation test, and (e) data acquisition system.

Table 4: Experimental instrument properties

Type	Product description	Accuracy
Temperature sensors	KYW-TC, Kunlunyuanyang, Beijing, China	±0.05°C
Temperature inspection instrument	Kunlunyuanyang, Beijing, China	±0.05% F.S
Eddy current displacement sensor	ML33-01-00-03, Milang, Shenzhen, China	0.05 μm
Displacement inspection instrument	XSAE-CHVB1M2V0, Milang, Shenzhen, China	±0.05% F.S

Table 5: Parameters design of material preparation and spraying process

No.	c_g (%)	m_s (g)	p_z (mL/min)
P1	20	0.1	1,500
P2	20	0.2	1,125
P3	20	0.3	1,200
P4	15	0.1	1,200
P5	15	0.2	1,500
P6	15	0.3	1,125
P7	10	0.1	1,125
P8	10	0.2	1,200
P9	10	0.3	1,500

dissipation. The properties of the instruments are shown in Table 2.

2.2 Thermal characteristics of graphene-coated ball screws

Due to the excellent thermal property of graphene and silver powder, the heat dissipation can be enhanced thereby reducing the temperature rise. Therefore, the thermal performance of the ball screw was improved. The cooling mechanism is shown in Figure 2, where Q_N

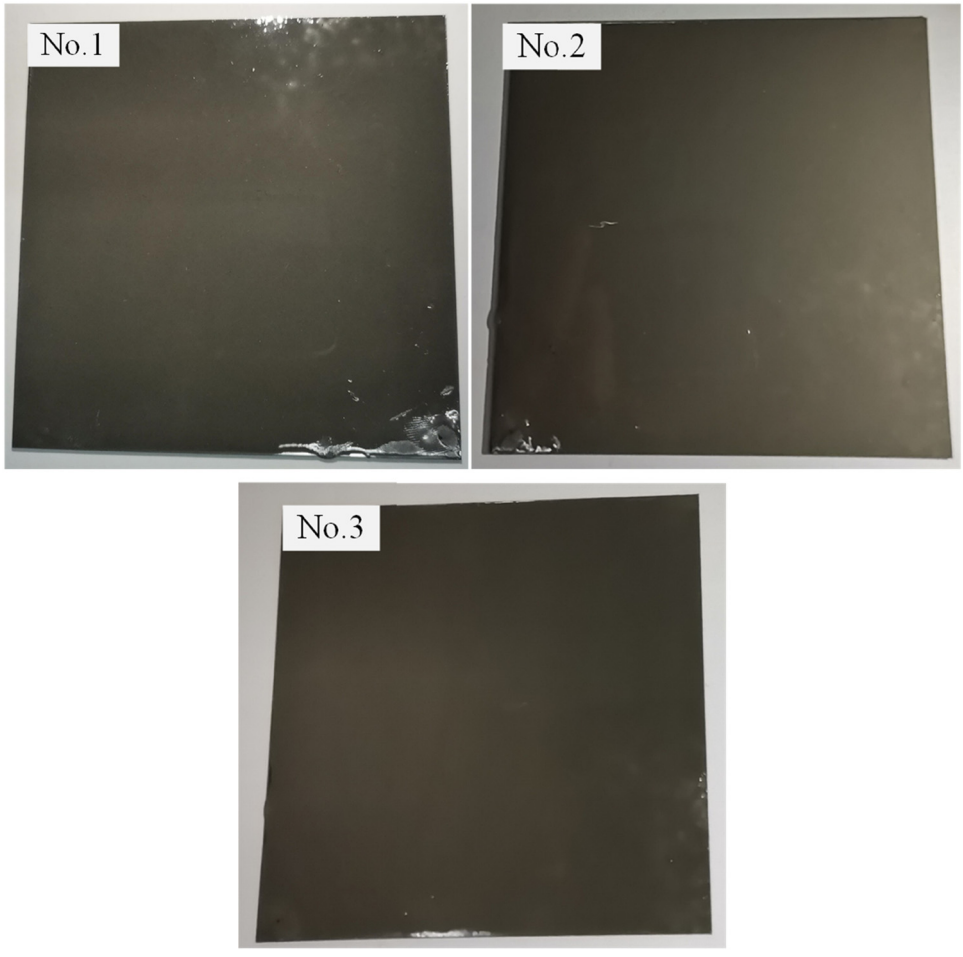

Figure 5: Coated samples.

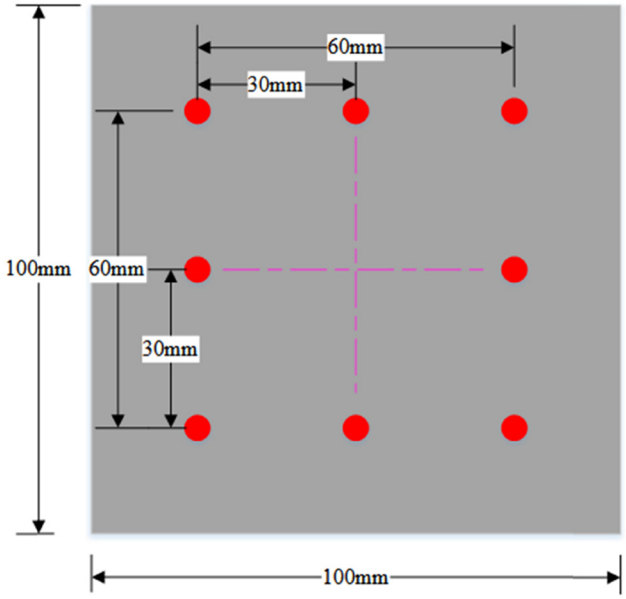

Figure 6: Position of measuring points.

is the heat generation rate of the nut, Q_C is the convective heat transfer, and Q_R is the radiative heat transfer. The nano coating was beneficial in temperature reduction of the ball screw by enhancing radiation heat dissipation, and thermal deformation can be effectively reduced. The coated ball screw has the advantage of adaptability to thermal deformation without complicated control and calculation.

SEM observation was employed to obtain the state representation and graphene distribution of the nano coating. The samples with good interface conditions after cutting and polishing were selected to prepare for the SEM images shown in Figure 3. From the SEM images, it is indicted that graphene presented a relatively even distribution. The advantages of graphene and nano silver powder with high thermal conduction were adopted to realize the high efficiency transmission of heat flow. Due to the thermal channels formed by graphene depicted in Figure 3(b), the heat generated during operation can be transferred to the environment more effectively resulting in the reduction in temperature and thermal deformation of the ball screw.

2.3 Experimental procedure

To validate the effectiveness of this method and obtain the optimal material ratio and spraying process, the orthogonal experiment was designed and carried out on our self-design test bench (Table 3), which allowed for collecting both the data of temperature and thermal deformation continuously and synchronously. The experimental setup is illustrated in Figure 4. The prepared ball screw with nano coating was driven at a speed of 1,000 rpm. Simultaneously, the temperature of the fixed bearing, supported bearing, ambient, and nut were collected using temperature sensors. Thermal deformation of the ball screw in axial direction was measured using the eddy current displacement sensor. The properties of the instruments are shown in Table 4.

Experiments on the ball screw with different coatings were carried out at the same working condition, and the ambient temperature was selected as the initial temperature. Based on the data acquisition system of LABVIEW, both the real-time temperature and thermal deformation were collected on a computer by the data acquisition card

Table 7: Thickness of coatings

Nozzle flow (mL/min)	Average thickness (μm)
1,500	169.63
1,200	158.50
1,125	150.75

Table 6: Thickness measurement results of samples

	Nozzle flow (mL/min)	Thickness of measuring points (μm)								
		A1	A2	A3	A4	A5	A6	A7	A8	Mean
Uncoated	1,500	928	926	927	930	936	936	931	927	930
	1,200	932	937	933	928	928	928	927	932	931
	1,125	932	932	926	927	933	927	936	935	931
Coated	1,500	1,109	1,080	1,111	1,118	1,115	1,062	1,095	1,108	1,100
	1,200	1,071	1,050	1,104	1,089	1,072	1,088	1,125	1,114	1,089
	1,125	1,060	1,066	1,065	1,110	1,093	1,077	1,095	1,088	1,082

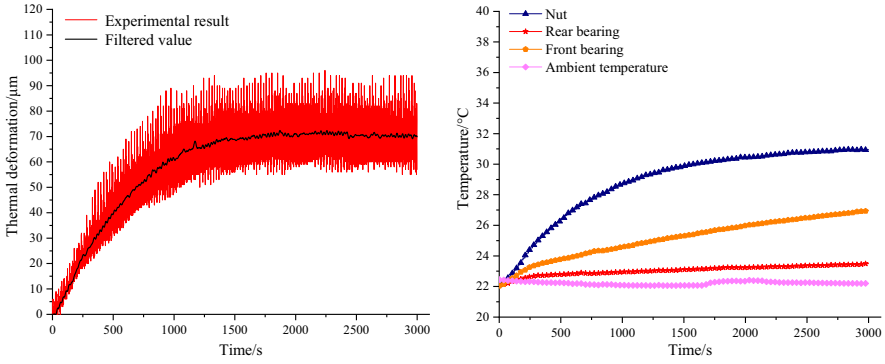
Experimental result
Filtered value
Thermal deformation/μm
Time/s
Nut
Rear bearing
Front bearing
Ambient temperature
Temperature/°C
Time/s

a)

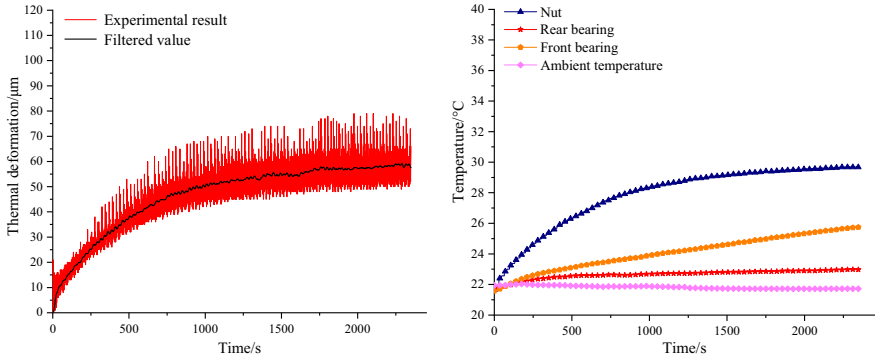
Experimental result
Filtered value
Thermal deformation/μm
Time/s
Nut
Rear bearing
Front bearing
Ambient temperature
Temperature/°C
Time/s

b)

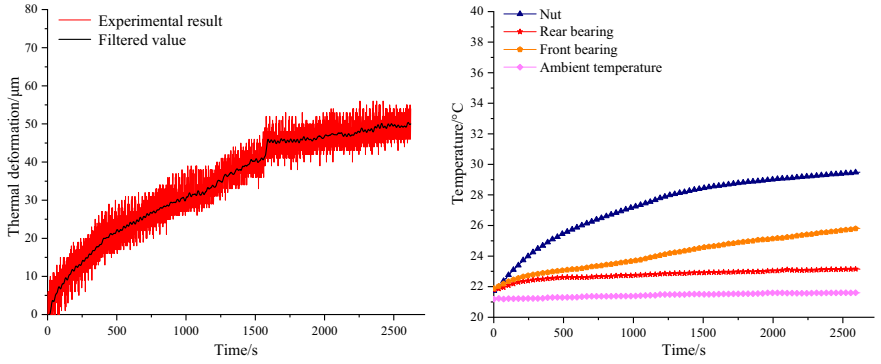
Experimental result
Filtered value
Thermal deformation/μm
Time/s
Nut
Rear bearing
Front bearing
Ambient temperature
Temperature/°C
Time/s

c)

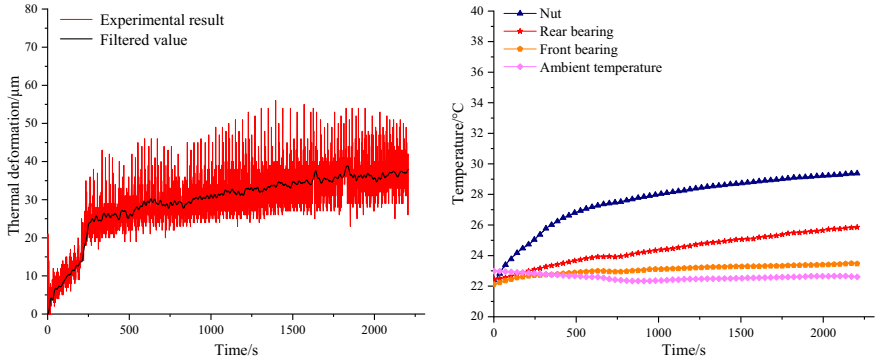
Experimental result
Filtered value
Thermal deformation/μm
Time/s
Nut
Rear bearing
Front bearing
Ambient temperature
Temperature/°C
Time/s

d)

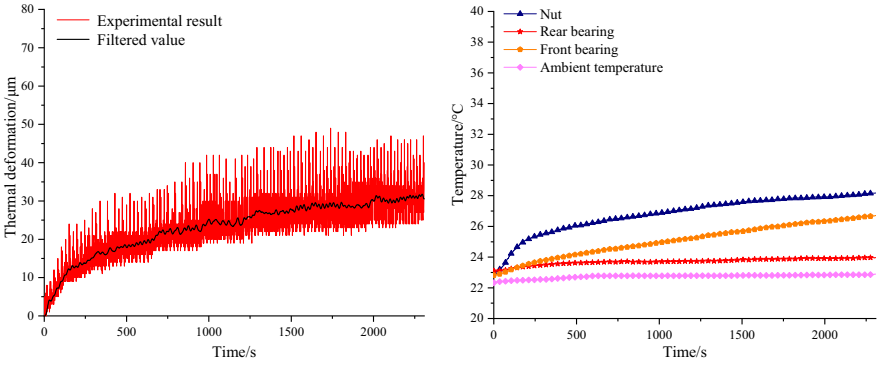
Experimental result
Filtered value
Thermal deformation/μm
Time/s
Nut
Rear bearing
Front bearing
Ambient temperature
Temperature/°C
Time/s

e)

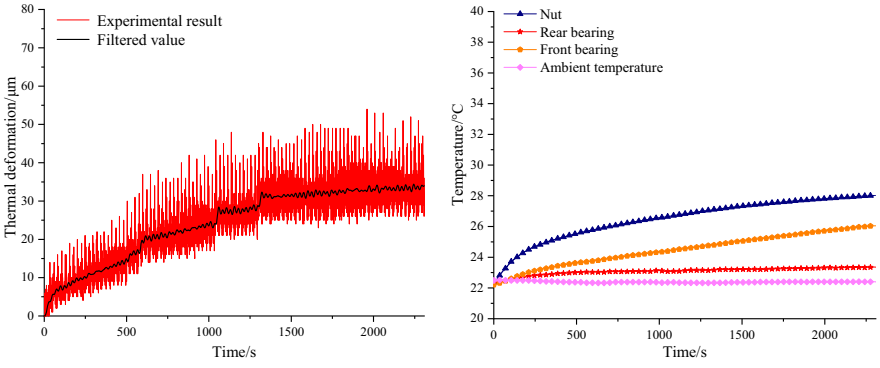
Experimental result
Filtered value
Thermal deformation/μm
Time/s
Nut
Rear bearing
Front bearing
Ambient temperature
Temperature/°C
Time/s

f)

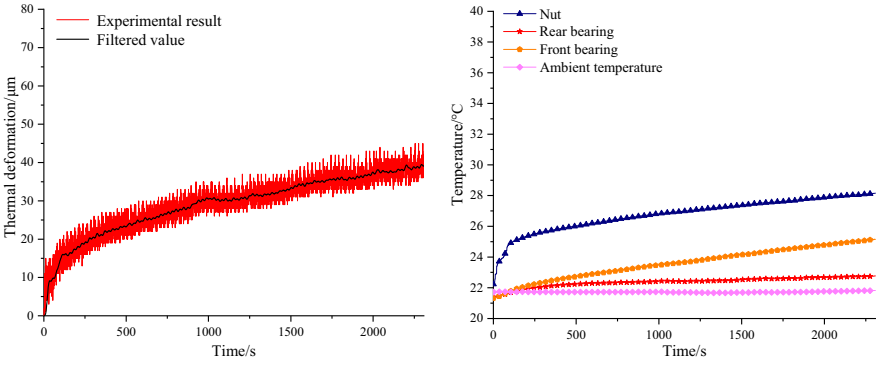
Experimental result
Filtered value
Thermal deformation/μm
Time/s
Nut
Rear bearing
Front bearing
Ambient temperature
Temperature/°C
Time/s

g)

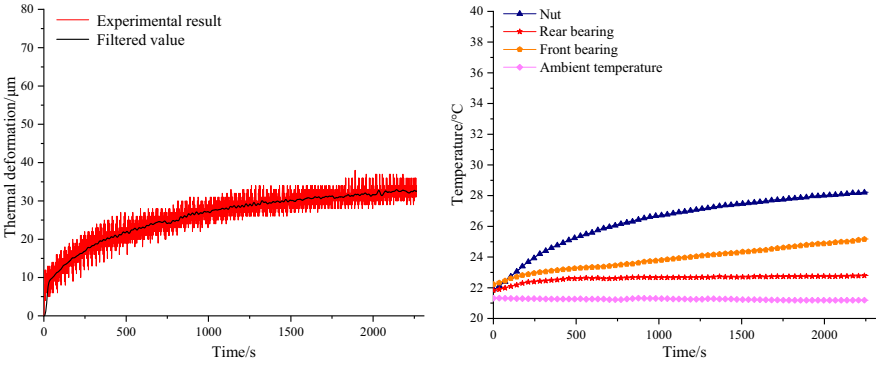
Experimental result
Filtered value
Thermal deformation/μm
Time/s
Nut
Rear bearing
Front bearing
Ambient temperature
Temperature/°C
Time/s

h)

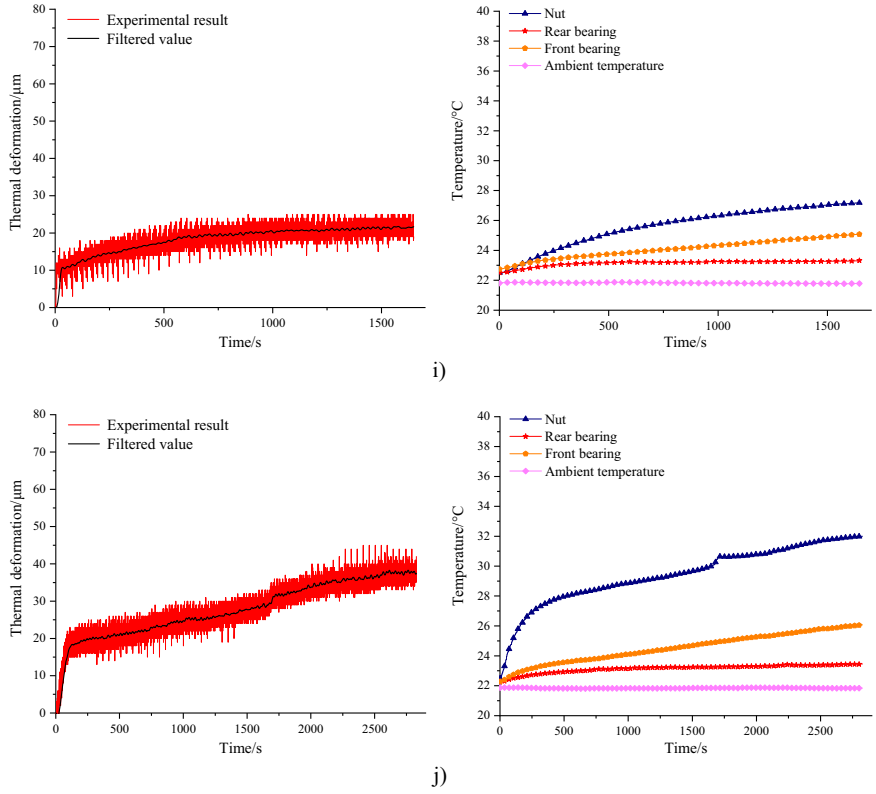

Figure 7: Experimental results of temperature and thermal deformation: (a) O1, (b) P1, (c) P2, (d) P3, (e) P4, (f) P5, (g) P6, (h) P7, (i) P8, and (j) P9.

and serial port. Between each experiment, one day was needed to dry the coatings and cool the ball screw.

2.4 Orthogonal design

To study the influence of material ratio and nozzle flow of nano coating on the ball screw temperature rise and thermal deformation, orthogonal experiment was designed. In this article, the nozzle flow p_z, the quality of graphene m_s, and nano silver powder c_g were selected as the key design parameters of the nano coating. Thus, the orthogonal table $L_9(3^4)$ with three factors and three levels was employed to generate the samples, as shown in Table 5. The quality of silicone resin and nano silver powder was regarded as the total mass of nano coating, and graphene was considered as an additional additive.

According to the orthogonal design, nine experiments were carried out on the ball screw with different nano coatings. Additionally, the experiment on the ball screw without nano coating was also conducted in the same working condition as a comparison.

2.5 Characterization of coating thickness

The performance of nano graphene coating can be influenced by spraying process. Thus, the relationship between coating thickness and nozzle flow was considered to study the effect of spraying process on the heat transfer and heat dissipation performance of the nano coating. According to the orthogonal table in Section 2.4, three types of nozzle flow including 1,500, 1,200, and 1,125 mL/min were set to characterize the thickness of coating. Three stainless steel

Table 8: Experimental results of thermal performances

No.	T_m (°C)	Δu (μm)	t_d (min)
O1	30.95	70.3	48.3
P1	29.69	59	37.5
P2	29.42	49.4	42.0
P3	29.31	37.1	35.1
P4	28.41	32.9	47.6
P5	27.99	33.9	37.8
P6	28.46	41.2	45.8
P7	28.13	32.5	36.1
P8	27.09	21.7	26.0
P9	31.93	38	45.7

surfaces (100 mm × 100 mm) were prepared and sprayed using the three types of nozzle flow. During the spraying process, the same spraying condition was used in thickness characterization. The samples with nano coating were dried in the ambient environment, as shown in Figure 5.

To obtain the accurate thickness of each sample, the thickness of eight points were measured by micrometer (SH2005A5946, Weidu, Leqing, China). The average of eight measurement points was regarded as the thickness of this sample. The measurement points are illustrated in Figure 6.

3 Results and discussion

3.1 Experimental results

The results of the samples thickness under different nozzle flows are shown in Tables 6 and 7 according to the method proposed in Section 2.5. The result indicated that the increase in the samples thickness is correlated with the increase in the nozzle flow. In this article, the coating thickness of the samples can be approximated as the one on the ball screw.

In Section 2.4, orthogonal experiment was designed to obtain the material ratio and spraying process of nano coating with optimal thermal performance. After collecting the temperature and thermal deformation, the comparative experimental results of nine types of graphene-coated ball screws (P1–P9) and standard one (O1) are drawn in Figure 7. The obvious oscillation occurred when the axial thermal deformation was collected, that is because the ball screw test bench is affected by vibration during operation. To obtain the thermal deformation clearly, the low pass filtering was adopted.

From the results of the orthogonal experiment, it was concluded that nano coating had a positive effect on reducing the temperature rise and thermal deformation of the ball screw. Moreover, different thermal properties were developed by nano coating with different material ratios and spraying processes. The maximum temperature rise (T_m), maximum thermal deformation (Δu), and thermal balance time (t_d) were selected as the criteria for evaluating the thermal performance. The results of each experiment are summarized in Table 8.

Table 9: Optimized design parameters of nano coating

Parameters	m_s (g)	c_g (%)	p_z (mL/min)
Value	0.2	10	1,200

Table 10: Range analysis on thermal deformation

Level	c_g (%)	m_s (g)	p_z (mL/min)
1st	48.5	41.5	43.6
2nd	36.0	35.0	30.6
3rd	30.7	38.8	41.0
Range	17.8	6.5	13.0

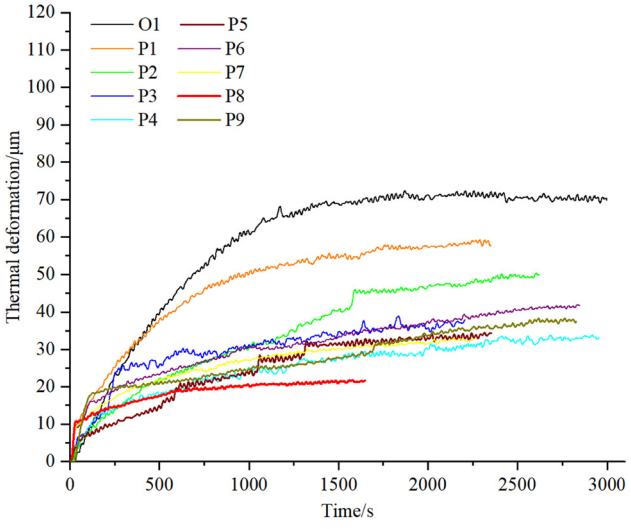

Figure 8: Comparative results of thermal deformation.

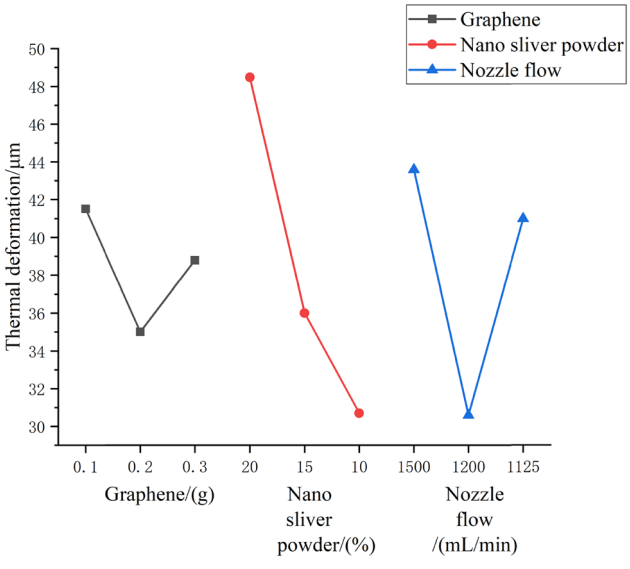

Figure 9: Influence of material ratio and spraying process on thermal deformation.

The thermal deformation of the ball screw with different nano coatings and the standard one are summarized in Figure 8. The minimal thermal deformation was found in the ball screw which was coated with P8 nano coating (Table 9). Therefore, it can be concluded that the P8 nano coating has the most excellent thermal performance. The maximum temperature rise, thermal deformation, and time to reach thermal balance of the ball screw with P8 coating decreased by 12.5, 69.1, and 46.3%, respectively.

3.2 Range analysis

In order to evaluate the influence of design parameters of nano coating on reducing the thermal deformation, the range analysis on thermal performance was conducted. The range value can indicate the sensitivity of the factors to the experimental results. A larger range value suggests that it has a greater impact on the experimental results. The results of the range analysis are shown in Figure 9 and Table 10.

Based on the analysis results, it was concluded that the thermal performance of the nano coating was influenced by the combination of three factors, and the proportion of nano silver powder had main effect on improvement of thermal performance. Thus, better thermal performance of nano coating can be ensured to improve positioning accuracy of the ball screw by using optimized material ratio and spraying process.

4 Conclusion

In this study, an optimization method of nano coating was conducted to improve its thermal performance. The nano coating used is composed of modified acrylic silicone resin, graphene, and nano silver powder. Due to the high thermal conductivity of graphene, the thermal channels can be formed by graphene which can diffuse the heat into the surrounding environment. Thus, material ratio (graphene and nano silver powder) and nozzle flow were considered as the factors which can influence the thermal performance of nano coating on the ball screw. The optimized nano coating formed by optimal material ratio and spraying flow was obtained by orthogonal experiment. The experimental data showed that the maximum temperature rise, thermal deformation and time to reach thermal balance of the ball screw with optimized coating decreased by 12.5, 69.1, and 46.3%, respectively, which proved that the optimized nano coating has promising thermal performance. In the future, the spraying process will be investigated to ensure that the coating is evenly coated on the ball screw surface aiming to further improve the thermal performance of the coating.

Acknowledgements: The authors would like to thank Mr Dzonu Ambrose Hanson for his kind proofreading.

Funding information: This study was supported by the National Natural Science Foundation of China (Grant Numbers: 51875008, 51505012, and 51575014), Royal Society *via* an International Exchange Programme (Grant Number: IEC\NSFC\191253), and the International Research Cooperation Seed Fund of Beijing University of Technology (Grant Number: 2021A10).

Author contributions: Xiangsheng Gao conceived the experiment, and wrote the manuscript as well. Kuan Zhang conducted the experiment. Tao Zan, Peng Gao, and Chaozong Liu conducted the data analysis and the English editing. Min Wang supervised this work and revised the manuscript. All authors have accepted responsibility for the entire content of this manuscript and approved its submission.

Conflict of interest: The authors state no conflict of interest.

Data availability statement: All data generated or analyzed during this study are included in this published article.

References

[1] Bryan J. International status of thermal error research. CIRP Ann Manuf Technol. 1990;39:645–56.
[2] Liu D, Lin P, Lin J, Wang C, Shiau T. Effect of environmental temperature on dynamic behavior of an adjustable preload double-nut ball screw. Int J Adv Manuf Technol. 2019;101(9–12):2761–70.
[3] Li Y, Su D, Cai X, Wu W, Zhang J, Zhao W. Temperature simulation and thermal equilibrium analysis of the ball screw feed drive system under various working conditions. Proc Inst Mech Eng C-J Eng Mech Eng Sci. 2020;234(24):4844–56.
[4] Xie H, Fang H, Cai W, Wan L, Huo R, Hui D. Development of an innovative composite sandwich matting with GFRP facesheets and wood core. Rev Adv Mater Sci. 2021;60(1):80–91.
[5] Li Z, Zhao C, Lu Z. Thermal error modeling method for ball screw feed system of CNC machine tools in *x*-axis. Int J Adv Manuf Technol. 2020;106(11–12):5383–92.

[6] Li T, Zhao C, Zhang Y. Prediction method of thermal errors of the screw system in lathes based on moving thermal network. Precis Eng. 2019;59:166–73.
[7] Chen Y, Chen J, Xu G. Screw thermal characteristic analysis and error prediction considering the two-dimensional heat transfer structure. Int J Adv Manuf Technol. 2021;115(7–8):2433–48.
[8] Gao X, Guo Y, Hanson D, Liu Z, Wang M, Zan T. Thermal error prediction of ball screws based on PSO-LSTM. Int J Adv Manuf Technol. 2021;116(5–6):1721–35.
[9] Yang H, Xing R, Du F. Thermal error modelling for a high-precision feed system in varying conditions based on an improved Elman network. Int J Adv Manuf Technol. 2020;106(1–5):279–88.
[10] Li T, Liu K. Dynamic model on thermally induced characteristics of ball screw systems. Int J Adv Manuf Technol. 2019;103(9–12):3703–15.
[11] Zapłata J, Pajor M. Piecewise compensation of thermal errors of a ball screw driven CNC axis. Precis Eng-J Int Soc Precis Eng Nanotechnol. 2019;60:160–6.
[12] Li T, Zhao C, Zhang Y. Adaptive on-line compensation model on positioning error of ball screw feed drive systems used in computerized numerical controlled machine tools. Proc Inst Mech Eng B J Eng Manuf. 2019;233(3):914–26.
[13] Liu J, Ma C, Wang S. Data-driven thermally-induced error compensation method of high-speed and precision five-axis machine tools. Mech Syst Signal Process. 2020;138:106538.
[14] Ju X, Lu J, Jin H. Study on heat transfer characteristics and thermal error suppression method of cylindrical giant magnetostrictive actuator for ball screw preload. Proc Inst Mech Eng B-J Eng Manuf. 2021;235(5):782–94.
[15] Shi H, He B, Yue Y, Min C, Mei X. Cooling effect and temperature regulation of oil cooling system for ball screw feed drive system of precision machine tool. Appl Therm Eng. 2019;161:114150.
[16] Voigt I, Navarro de Sosa I, Wermke B, Bucht A, Drossel W. Increased thermal inertia of ball screws by using phase change materials. Appl Therm Eng. 2019;155:297–304.
[17] Gao X, Qin Z, Guo Y, Wang M, Zan T. Adaptive method to reduce thermal deformation of ball screws based on carbon fiber reinforced plastics. Materials. 2019;12(19):3113.
[18] Gao X, Guo Y, Wang M, Zan T. Further study on thermal deformation reduction for CFRP-based improved ball screws. Adv Compos Lett. 2020;29:2633366X20917981.
[19] Gao X, Zhang K, Wang M, Zan T, Luo J. Thermally stimulated artificial muscles: Bio – inspired approach to reduce thermal deformation of ball screws based on inner – embedded CFRP. Rev Adv Mater Sci. 2021;60(1):541–52.
[20] Japar W, Sidik N, Saidur R, Asako Y, Yusof S. A review of passive methods in microchannel heat sink application through advanced geometric structure and nano fluids: current advancements and challenges. Nanotechnol Rev. 2020;9(1):1192–216.
[21] Bhat A, Budholiya S, Raj S, Sultan M, Hui D, Shah A, et al. Review on nanocomposites based on aerospace applications. Nanotechnol Rev. 2021;10(1):237–53.
[22] Zheng L, Xiong T, Shah K. Transparent nanomaterial-based solar cool coatings: synthesis, morphologies and applications. Sol Energy. 2019;193:837–58.
[23] Chen M, Li W, Tao S, Fang Z, Lu C, Xu Z. A pragmatic and high-performance radiative cooling coating with near-ideal selective emissive spectrum for passive cooling. Coatings. 2020;10(2):144.
[24] Cheng Z, Shuai Y, Gong D, Wang F, Liang H, Li G. Optical properties and cooling performance analyses of single-layer radiative cooling coating with mixture of TiO_2 particles and SiO_2 particles. Sci China-Technol Sci. 2021;64(5):1017–29.
[25] Niazi S, Sadaghiani A, Gharib G, Kaya V, Celik S, Kutlu O, et al. Bio-coated surfaces with micro-roughness and micro-porosity: next generation coatings for enhanced energy efficiency. Energy. 2021;222:119959.
[26] Sivanathan A, Dou Q, Wang Y, Li Y, Corker J, Zhou Y, et al. Phase change materials for building construction: an overview of nano-/micro-encapsulation. Nanotechnol Rev. 2020;9(2):896–921.
[27] Zhang Y, Zhu Y, Yang J, Zhai X. Energy saving performance of thermochromic coatings with different colors for buildings. Energy Build. 2020;215:109920.
[28] Yi Y, Jiang Y, Li Q, Deng C, Ji X, Xue J. Development of super road heat-reflective coating and its field application. Coatings. 2019;9(12):802.
[29] Wang C, Sun X, Guo T, Gao Z, Wang X. Investigations on cooling effects of prepared pavement coatings using the Grubbs method and linear regression analysis. Road Mater Pavement Des. 2019;20(1):171–86.
[30] Chen Y, Hu K, Cao S. Thermal performance of novel multilayer cool for asphalt pavements. Materials. 2019;12(12):1903.
[31] Tarawneh M, Saraireh S, Chen R, Ahmad S, Al-Tarawni M, Yu L, et al. Mechanical reinforcement with enhanced electrical and heat conduction of epoxy resin by polyaniline and graphene nanoplatelets. Nanotechnol Rev. 2020;9(1):1550–61.
[32] Chen L, Shen Y, Yi H, Liu Z, Song Q. Mathematical modeling of heat transfer in GO-doped reinforce polymer for anti-/deicing of wind turbines. Int Commun Heat Mass Transf. 2021;123:105235.
[33] Chen M, Pang D, Chen X, Yan H. Enhancing infrared emission behavior of polymer coatings for radiative cooling applications. J Phys D-Appl Phys. 2021;54(29):295501.
[34] Du M, Jing H, Gao Y, Su H, Fang H. Carbon nanomaterials enhanced cement-based composites: advances and challenges. Nanotechnol Rev. 2020;9(1):115–35.
[35] Cheng Z, Wang F, Wang H, Liang H, Ma L. Effect of embedded polydisperse glass microspheres on radiative cooling of a coating. Int J Therm Sci. 2019;140:358–67.
[36] Kolas T, Royset A, Grandcolas M, ten Cate M, Lacau A. Cool coatings with high near infrared transmittance for coil coated aluminium. Sol Energy Mater Sol Cell. 2019;196:94–104.
[37] Zhang H, Fan D. Improving heat dissipation and temperature uniformity in radiative cooling coating. Energy Technol. 2020;8(5):1901362.
[38] Kang H, Qiao Y, Li Y, Qin W, Wu X. Keep cool: polyhedral ZnO@ZIF-8 polymer coatings for daytime radiative cooling. Ind Eng Chem Res. 2020;59(34):15226–32.

[39] Chen G, Wang Y, Qiu J, Cao J, Zou Y, Wang S, et al. Robust inorganic daytime radiative cooling coating based on a phosphate geopolymer. ACS Appl Mater Interfaces. 2020;12(49):54963–71.
[40] Guo Y, Gao X, Wang M, Zan T. Bio-inspired graphene-coated ball screws: novel approach to reduce the thermal deformation of ball screws. Proc Inst Mech Eng C J Mech Eng Sci. 2021;235(5):789–99.
[41] Behdinan K, Moradi-dastjerdi R, Safaei B, Qin Z, Chu F, Hui D. Graphene and CNT impact on heat transfer response of nanocomposite cylinders. Nanotechnol Rev. 2020;9(1):41–52.
[42] Liu C, Huang X, Wu Y, Deng X, Zheng Z, Xu Z, et al. Advance on the dispersion treatment of graphene oxide and the graphene oxide modified cement-based materials. Nanotechnol Rev. 2021;10(1):34–49.